MOLECULAR IMAGING AND BIOLOGY

Mol Imaging Biol (2015) 17:643–651
DOI: 10.1007/s11307-015-0830-z

Published Online: 11 February 2015

RESEARCH ARTICLE

Combined Fluorescence and Magnetic Resonance Imaging of Primary Macrophage Migration to Sites of Acute Inflammation Using Near-Infrared Fluorescent Magnetic Nanoparticles

Sungmin Kang,[5] Ho Won Lee,[1] Young Hyun Jeon,[1,8] Thoudam Debraj Singh,[1] Yun Ju Choi,[1] Ji Young Park,[3] Jun Sung Kim,[7] Hyunseung Lee,[6] Kwan Soo Hong,[6] Inkyu Lee,[4] Shin Young Jeong,[1] Sang-Woo Lee,[1] Jeoung-Hee Ha,[2] Byeong-Cheol Ahn,[1] Jaetae Lee[1,9]

[1]*Department of Nuclear Medicine, Kyungpook National University School of Medicine, 50 Samduk-dong 2-ga, Chung Gu, Daegu, 700-721, South Korea*
[2]*Department of Pharmacology, Kyungpook National University School of Medicine, Daegu, South Korea*
[3]*Department of Pathology, Kyungpook National University School of Medicine, Daegu, South Korea*
[4]*Department of Endocrinology, Kyungpook National University School of Medicine, Daegu, South Korea*
[5]*Department of Nuclear Medicine, Catholic University of Daegu School of Medicine, Gyeongsan-si, South Korea*
[6]*Division of MR Research, Korea Basic Science Institute, Daejeon, South Korea*
[7]*R&D Center, Biterials, Goyang-si, 410-050, South Korea*
[8]*Leading-edge Research Center for Drug Discovery and Development for Diabetes and Metabolic Disease, Kyungpook National University Hospital, 807 Hogukro, Bukgu, Daegu, 702-210, South Korea*
[9]*Daegu-Gyeongbuk Medical Innovation Foundation (DGMIF), 80 Cheombok-ro, Dong-gu, Daegu, 701-310, Korea*

Abstract

Purpose: This study aimed to track the migration of primary macrophages labeled with near-infrared (NIR) fluorescent magnetic nanoparticles toward chemically induced acute inflammatory lesions in mice and to visualize the effect of anti-inflammatory drugs on macrophage migration using combined fluorescence and magnetic resonance imaging (FLI/MRI).

Procedures: Primary macrophages were labeled with NIR fluorescent magnetic nanoparticles, and labeled cells were injected into mice intravenously. One day later, inflammation was induced by subcutaneous injection of 1 % carrageenan (CG) solution to footpads of the right hind leg, and phosphate-buffered saline (PBS) as control treatment was subcutaneously injected to footpad of the left hind leg. To evaluate the effect of drug treatment on macrophage migration, a single dose of dexamethasone (DEX) was intraperitoneally administered to the mice

Sungmin Kang and Ho Won Lee contributed equally to this work.
Electronic supplementary material The online version of this article (doi:10.1007/s11307-015-0830-z) contains supplementary material, which is available to authorized users.

Correspondence to: Young Jeon; *e-mail:* jeon9014@gmail.com, Jaetae Lee; *e-mail:* jaetae@knu.ac.kr

immediately after the induction of inflammation and was followed by combined FLI/MRI at predetermined time points.
Results: No difference in cellular viability or phagocytic activity was observed between the labeled and parent macrophages. *In vivo* optical imaging revealed an increase in FLI signals in CG-injected footpads in a time-dependent manner, but not in PBS-treated footpads. DEX treatment inhibited the migration of the labeled macrophages to the CG-injected footpads, with relative decreases in FLI activity. In accordance with FLI, T_2*-weighted MR images showed hypo-intense signals in the CG-injected footpads but not in the PBS-injected footpads. The DEX-treated mice did not show a dark signal loss zone on MR images in the CG-treated paw.
Conclusions: We successfully tracked the migration of macrophages to inflammatory lesions using both FLI and MRI with NIR fluorescent magnetic nanoparticles and demonstrated the inhibitory effects of DEX on macrophage migration to inflammation sites.

Key words: Macrophage migration, Combined fluorescence and magnetic resonance imaging, Acute inflammation, Near-infrared fluorescent magnetic nanoparticles

Introduction

Macrophages are important immune cells that are implicated in the onset, progression, and manifestation of various pathologic processes, such as formation of malignant tumors and inflammatory diseases [1]. Macrophages act as hosts and reservoirs for pathogens and produce pro-inflammatory or pro-angiogenic mediators [2, 3]. Numerous studies have shown that modulating macrophage recruitment represents a promising therapeutic strategy for controlling inflammatory diseases [4, 5].

The detection of inflammatory processes is essential for managing patients and for the successful treatment of acute and chronic inflammatory diseases after early diagnosis. However, there are still many obstacles impeding capitulation of the complex biological processes involved in inflammatory diseases. Therefore, the need for robust and quantitative techniques to assess advanced inflammation and therapeutic interventions *in vivo* has greatly increased. Noninvasive *in vivo* imaging methods have been proposed to allow better localization, visualization, and quantification of inflammation-related processes for preclinical and clinical applications.

Tracking macrophage migration is very important for better understanding various inflammation-related events and has been widely investigated using an assortment of molecular imaging techniques, including optical imaging [6, 7], nuclear medicine imaging [8, 9], and magnetic resonance imaging (MRI) [3, 10, 11]. Most of these reports have used a single modality to visualize the distribution and migration of macrophages, but there are drawbacks to using a single imaging modality for tracking macrophages. Although optical imaging methods, such as fluorescence (FLI) or bioluminescence imaging, have high sensitivity with low background, which enables tracking of the early distribution of infused macrophages, these methods cannot be used in large animals because of their depth limitations. MRI has been successfully applied to visualize the migration of immune cells and provides fast noninvasive imaging with high spatial resolution. But, it should require the millimolar amounts of contrast agents and there exist artifacts because of inaccurate coil sensitivities. Nuclear medicine imaging can not only provide high sensitivity without depth limitation but can also allows pharmacodynamics (PD)/pharmacokinetics (PK) study due to ability of quantitative analysis. However, this imaging modality has low spatial resolution and concern about radiation safety. Because there are several limitations associated with using a single imaging modality to visualize the entire process of macrophage migration *in vivo*, a multimodal imaging strategy is required to overcome these obstacles. Multimodal imaging strategies with individual imaging tools can be used to visualize infused macrophages at different, specific, and sequential phases of the pathological process by exploiting the best features of each modality.

In this study, we attempted to adopt a near-infrared (NIR) fluorescent magnetic nanoparticle that may enable visualization of early distribution as well as subsequent tracking of macrophages in an inflammation model. Previously, the use of this multimodal imaging nanoparticle allowed noninvasive imaging with both FLI and MRI in a living organism, as these biocompatible silica-coated magnetic nanoparticles contain a NIR fluorescence dye within a silica shell and a magnetic core [12–16]. For this study, we first tracked the migration of primary macrophages using both FLI and MRI in living mice with acute inflammation induced by an injection of carrageen (CG) solution into the footpad. Second, we further attempted to visualize the impact of dexamethasone (DEX), a potent steroid hormone with anti-inflammatory effects, on the migration of macrophages to inflammatory lesions in mice with CG-induced inflammation.

Materials and Methods

Additional information is reported in the supplementary data.

Animals

Specific pathogen-free, 6-week-old, immunocompetent Balb/c mice were obtained from SLC, Inc. (Shizuoka, Japan). All animal experimental procedures were conducted in strict accordance with the appropriate institutional guidelines for animal research. The protocol was approved by the Committee on the Ethics of Animal Experiments of the Kyungpook National University (permit number: KNU 2012-43).

In Vivo Study

The animal experimental procedure is illustrated with a schematic diagram as shown in Supplementary Fig. 3. Briefly, macrophages labeled with fluorescent magnetic nanoparticles were injected into mice via the tail vein, and the mice were divided into two groups on day 1 after transfer of the labeled cells: the vehicle group and the DEX-treated group (n=5 mice per group). Before inflammation induction, baseline activity of FLI was acquired, and then, phosphate-buffered saline (PBS) and 1 % CG solution (50 μl per mouse) for induction of inflammation were subcutaneously injected into the left and right footpads, respectively. To evaluate the therapeutic effects of DEX treatment, mice received either a single IP dose of 30 mg/kg DEX or a vehicle control immediately after CG injection. Combined FLI and MRI were performed to monitor the migration of labeled macrophages at 3, 6, and 24 h post-inflammation induction. Mice were sacrificed when all imaging procedure of combined MRI and FLI was completed (at 24 h post-inflammation induction). Organs of interest were excised and followed by *ex vivo* FLI imaging.

In Vivo MRI

All animals (n=6 mice per group) were anesthetized with 1–1.25 % (v/v) isoflurane in a 3:7 mixture of O_2/N_2O during the MRI scan. T_2-W and T_2^*-W MR images were acquired using a 4.7-T animal MRI system with a quadrature birdcage RF coil (35 mm inner diameter) for signal transmission and reception. The following parameters were used: a turbo RARE pulse sequence (echo time (TE)/repetition time (TR)=40/3500 ms, matrix size=256×256, field of view (FOV)=40×30 mm^2, slice thickness=1, number of slices=3, number of averages=4 for T_2-W MRI) and a fast low angle shot (FLASH) pulse sequence (TE/TR=8/190 ms, matrix size=256×256, FOV=40×30 mm^2, slice thickness=1 mm, number of slices=3, number of averages=4 for T_2^*-W MRI).

Optical Imaging

Before beginning optical imaging, we tested the best optimal condition of filter set for NIR675 nanoparticle. Using several filter set (Ex/Em, 620/710, 640/710, and 660/710) which is compatible with NIR675 fluorescent dye, raw images were obtained. The acquired raw data were spectrally unmixed to determine the auto-fluorescence (from skin and food uptake, etc.) and real signal of NIR675 from living mouse with spectrum analysis system of Living Image 4.2 software and IGOR image analysis software. Filter set of Ex/Em, 660 nm/710 nm, was finally chosen to separate real signal of NIR675 nanoparticles from tissue auto-fluorescent signal. All *in vivo* FLI was obtained with the following settings: Ex/Em, 660 nm/710 nm; exposure time, 2 s; f/stop, 2; binning, 4; and field of view, 13.1.

In vivo NIR fluorescent optical imaging was performed at before (as baseline, before inflammation induction) and 3, 6, and 24 h post-transfer of labeled cells using the IVIS system (Caliper, Alameda, CA). After all imaging procedures of combined MRI and FLI at 24 h post-inflammation induction, the mice were killed and the major organs were excised, including the heart, lungs, liver, stomach, spleen, kidneys, intestines, and right and left paws. The excised organs were then imaged *ex vivo*. ROIs were drawn over the areas of interest in each mouse for quantitative analysis.

Histopathological Analysis

Footpads were excised 24 h after inflammation induction and preserved in 10 % formalin until use. All inflammatory tissues were embedded in paraffin, sectioned into 5-μm-thick sections, and stained with hematoxylin and eosin.

For deparaffinization, tissue slides were incubated for 20 min at 55 °C and rinsed three times with 1× PBS. Deparaffinized tissue slides were incubated with 4,6-diamidino-2-phenylindole (DAPI; Fluka, Buchs, St. Gallen, Switzerland) for 15 min at room temperature to stain the cell nuclei. These tissue slides were then washed twice with PBS and mounted using a ProLong Antifade Kit (Molecular Probes; Invitrogen, Grand Island, NY). Fluorescent signals of these tissues were captured and analyzed using Leica TCS SP2 (Leica, Wetzlar, Germany).

Statistical Analysis

In vitro assay such as fluorescence-activated cell sorting (FACS) analysis, cell counting kit (CCK) assay, cell labeling efficiency assay, and phagocytic activity assay was performed at least three times, and the data were represented as the mean±SD of three independent experiments. Combined MRI and FLI study as well as PET/CT imaging *in vivo* was also performed for three times, and the data are expressed as the mean±SD of three independent experiments (n=5 mice). Statistical significance was determined using an unpaired Student's t test. P values of <0.05 were considered statistically significant.

Results

In Vitro Characterization of Labeled Macrophage

The phenotype markers of the isolated peritoneal macrophages were evaluated by FACS analysis using CD86, CD11b, and F4/80 antibodies, which are specific molecules associated with macrophage maturation. These surface markers were highly expressed in isolated peritoneal macrophages (Supplementary Fig. 4). Gene expression of

CD4, a negative marker, was not detected in the isolated macrophages. FACS analysis showed that almost 100 % of cells in the labeled macrophage population exhibited the NIR675-specific signal (Fig. 1a). *In vitro* FLI and MR imaging of the tube phantom containing labeled cells revealed an increase in FLI activity (Fig. 1b) and dark signal loss in T_2-weighted MRI by increases in cell number (Fig. 1c).

Effects of Cell Labeling on Macrophage Proliferation and Phagocytic Function

There was no significant difference in cellular proliferation activity between nonlabeled and labeled macrophages (Fig. 2a). When the macrophages were co-incubated with 7-aminoactinomycin D (AAD)-positive *Escherichia coli* at 37 °C, there was no difference in phagocytic activity between

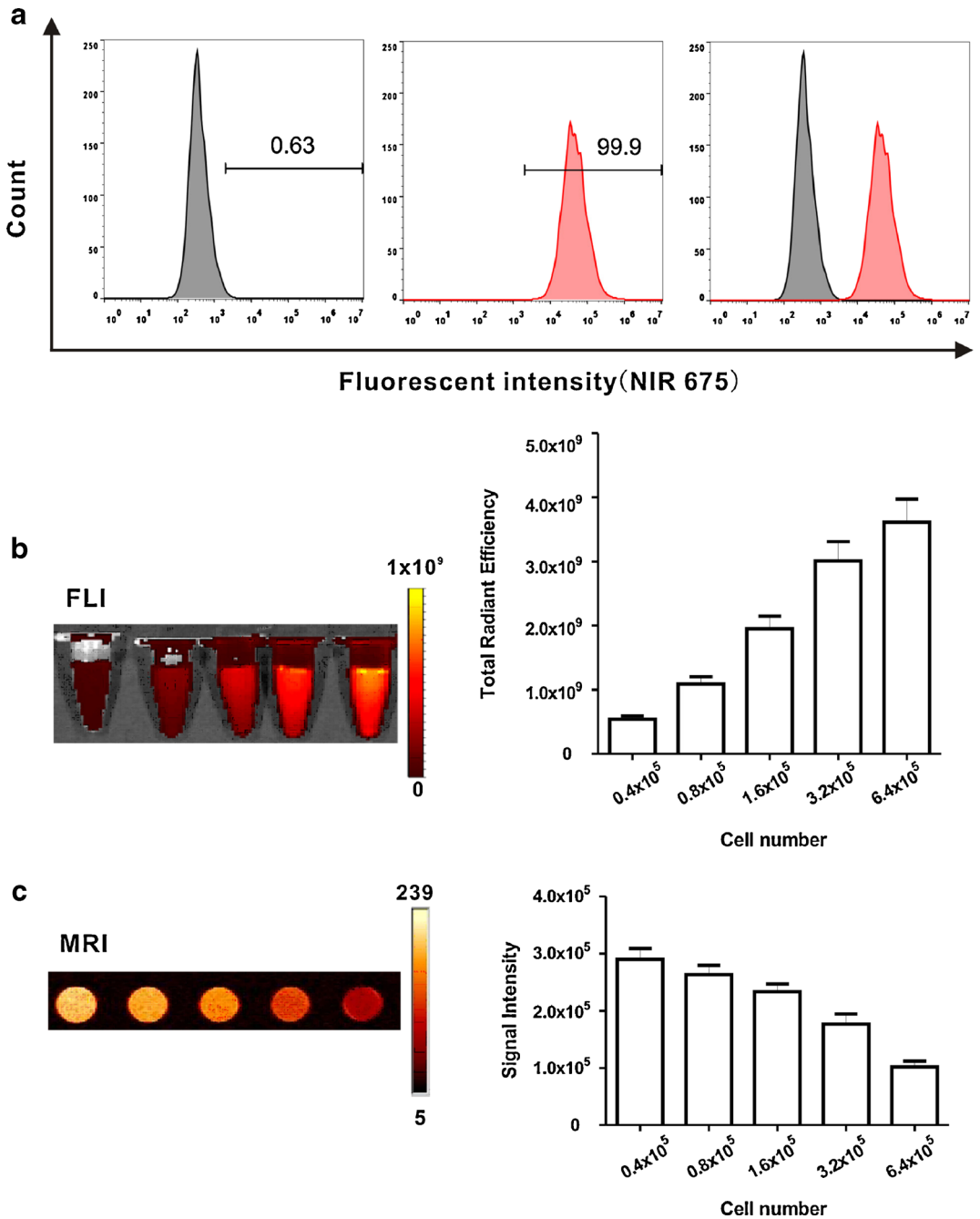

Fig. 1 NIR fluorescent magnetic nanoparticle labeling of primary macrophages and *in vitro* FLI/MRI. **a** Isolated macrophages were labeled with fluorescent magnetic nanoparticles, and the labeling efficiency was determined using flow cytometry. FACS analysis showed that 100 % of the macrophage population displayed strong fluorescent signals. **b** Combined FLI and **c** MRI of tube phantoms containing labeled cells. Both fluorescent and negative contrast in T_2-weighted MR images increased in a cell number-dependent manner.

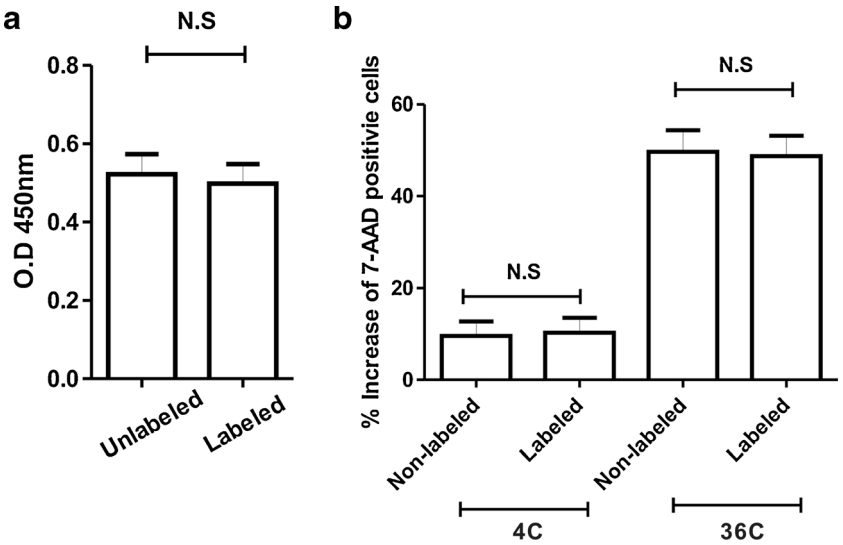

Fig. 2 The effect of NIR fluorescent magnetic nanoparticles on the cellular function of primary macrophages. **a** Cell viability of nonlabeled and nanoparticle-labeled macrophages was determined using a CCK assay 2 days after cell seeding. **b** Measurement of the phagocytic activity of unlabeled and nanoparticle-labeled macrophages at 4 and 37 °C. The *Y-axis* indicates a relative increase in the percentage of 7-AAD-positive cells. *7-AAD* 7-aminoactinomycin D, *N.S.* not significant.

the two groups (Fig. 2b, 49.6±4.6 and 48.7±4.4 % in nonlabeled and labeled macrophages, respectively). Complete inhibition of phagocytic activity was observed at 4 °C in both types of macrophages (9.5±3.1 and 10.2±3.2 %, in nonlabeled and labeled macrophages, respectively).

In Vivo Imaging of CG-Induced Inflammatory Lesions with 2-Deoxy-2-[^{18}F]fluoro-D-glucose PET/CT

PET/CT with 2-deoxy-2-[^{18}F]fluoro-D-glucose [^{18}F]FDG, a widely used imaging modality to diagnose inflammation in living subjects, was used to verify formation of inflammatory lesion [17, 18]. Small animal PET/CT imaging with [^{18}F]FDG demonstrated intense uptake of the radiotracer in the CG-injected footpads but not in the PBS-injected footpads (Supplementary Fig. 2a). Focal increased uptake in inflammatory lesions was evident at 3 h following inflammation induction, and the signal intensity gradually increased until 24 h (Fig. 2b, 0.27±0.08, 0.63±0.09, and 0.81±0.16 % ID/g at 3, 6, and 24 h, respectively). Histological evaluation of the swollen tissue further demonstrated diffuse infiltration of acute inflammatory cells at 24 h after inflammation induction (Supplementary Fig. 5, white arrows indicate neutrophil and macrophage).

Combined FLI and MRI of Macrophage Migration to Inflammatory Lesions

In vivo FLI revealed the early distribution of the infused macrophages into the lung within 1 h post-injection of the labeled macrophages (data not shown), and the localization of infused macrophages in the lung was observed up to 24 h after injection (Fig. 3a, mice in vehicle and DEX groups before inflammation induction).

At 3 h after inflammation induction, strong FLI signals were first observed in the CG-injected footpads but not in the PBS-injected footpads (Fig. 3a, upper panel, indicating the vehicle group). FLI signals of the inflammatory lesions peaked at 6 h, and there was a decrease in FLI signals at 24 h. The relative increase in FLI signals in the inflammatory lesions was 63.5 ±48.7, 326.0±14.1, and 282.5±62.9 % at 3, 6, and 24 h, respectively (Fig. 3b). *In vivo* FLI imaging was performed at very early times such as 0 and 2 h after inflammation induction, but signals from migrated macrophage were not detected at inflammatory lesions during these time points (data not shown).

T_2- and T_2^*-weighted MRI scans revealed hypo-intense signals (indicating infiltration of labeled macrophages) in the inflammatory lesions at both 6 and 24 h after inflammation induction (Fig. 3c, upper panel, indicating the vehicle group). In contrast to FLI, a significant signal change in the inflammatory lesions on T_2- and T_2^*-weighted imaging was not observed at early time point such as 3 h.

Evaluation of Effects of DEX on Macrophage Migration to Inflammatory Lesions with Combined FLI and MRI

DEX treatment resulted in significant inhibition of macrophage migration to the inflammatory lesions when compared with the vehicle group as demonstrated by *in vivo* imaging up to 24 h (Fig. 3a, bottom panel). The relative increases in FLI signals from the inflammatory lesions in DEX-treated mice were 14.75 ±11.29, 13.0±26.39, and 183.3±12.8 % at 3, 6, and 24 h, respectively, which are significantly lower than the values in

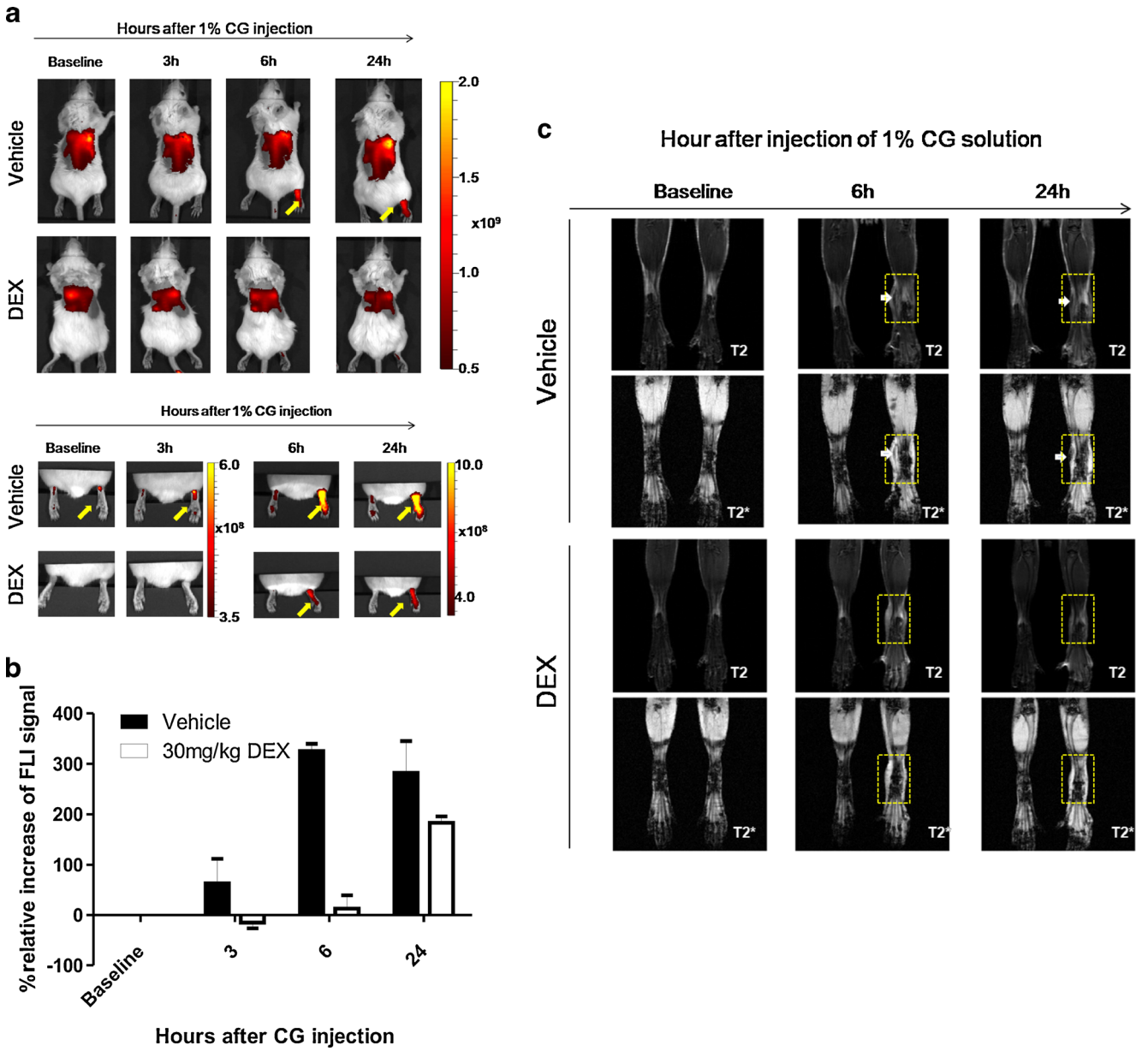

Fig. 3 *In vivo* tracking of macrophages labeled with NIR fluorescent magnetic nanoparticles using combined FLI and MRI. **a** Tracking of primary macrophage migration with FLI and **b** quantification of the FLI signal. **c** Coronal T_2-weighted and T_2*-weighted MR images depicting primary macrophage migration to the inflamed lesion. FLI was performed with the IVIS system at the designated times. MRI was performed with a small animal 4.7-T MRI. Strong FLI signals and hypo-intense signals at 1 % CG-induced inflammation sites are indicated with *arrows*. The relative increase (%) was expressed based on a comparison between the FLI signal of the CG-injected footpad and the FLI signal of the vehicle-treated footpad.

the vehicle-treated group ($P<0.01$, between vehicle and DEX-treated group). Similar to the findings for *in vivo* FLI, signal loss lesions were not detected in T_2- and T_2*-weighted MR imaging of DEX-treated mice at 6 h, and a hypo-intense signal was also not observed in the inflammatory lesions up to 24 h (Fig. 3c, bottom panel, indicating the 30 mg/kg DEX group).

Footpads were excised to perform both *ex vivo* FLI imaging and confocal microscopic imaging at 24 h post-inflammation induction, which was about 48 h after the transfer of labeled macrophages. *Ex vivo* imaging showed strong FLI signals in the CG-injected footpads in the vehicle-treated mice but not in DEX-treated mice (Supplementary Fig. 6). Consistent with the *ex vivo* FLI findings, confocal microscopic imaging revealed a focal accumulation of infused macrophages in inflammatory tissue excised from the vehicle-treated group but not in the inflammatory tissue excised from the DEX-treated group (Fig. 4).

Discussion

The diverse molecular and cellular events that occur in inflammatory disease are not clearly understood; therefore,

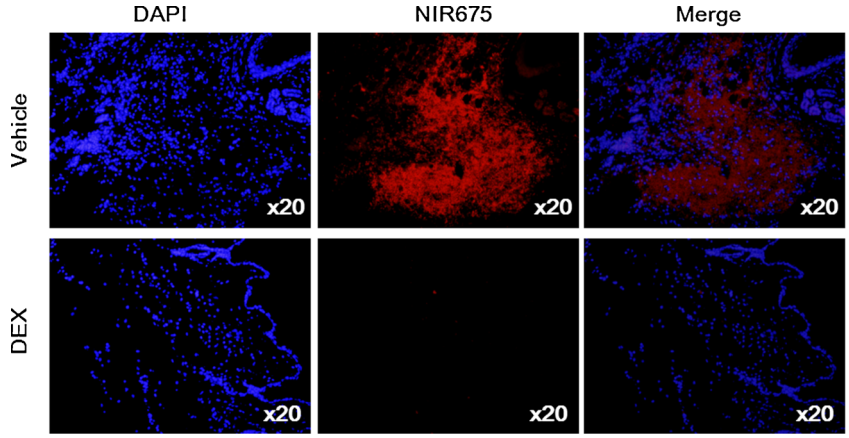

Fig. 4 Confocal microscopy images of the distribution of macrophages labeled with NIR fluorescent magnetic nanoparticles in inflamed tissue. *Red spots* indicate labeled macrophages.

further investigation is still needed using *in vivo* animal models of various inflammatory diseases. For this reason, noninvasive imaging methods, which include effective cell-labeling strategies and highly sensitive imaging techniques, need to be developed to explain the cellular interactions generated by inflammatory stimuli *in vivo*. Particularly, the development of an appropriate cell-labeling technique that does not affect cellular function and ensures stable, efficient labeling is mandatory.

The labeling technique with NIR fluorescent magnetic nanoparticles has several advantages over other labeling techniques. A previous report described tracking macrophage migration to inflamed lesions in an antigen-induced arthritis model with NIR fluorochrome-conjugated antibodies [19]. However, the use of cell surface markers for visualizing macrophages is not an appropriate approach because macrophages are not homogenous within a cell population. Recently, tracking macrophage migration to inflammatory lesions was attempted in mice using a cutaneous granuloma model with NIR fluorescent dye and a fluorescence-mediated tomography (FMT) imaging technique [6]. Although the localization and migration of macrophages was successfully visualized with FMT, this method cannot be applied to a large animal model or in clinical situations because of its depth limitations. Among various MR imaging agents used for cell tracking, iron oxide has also been applied to monitor macrophage migration in experimentally induced soft-tissue infections in mice [11]. Monitoring the early distribution of infused macrophages has still been a difficult challenge, although macrophage migration to inflamed lesions has been successfully monitored 1 day following infection induction.

In the current study, we demonstrated the feasibility of NIR fluorescent magnetic nanoparticles as a multimodal imaging probe to enable the tracking of macrophage migration toward acute inflammatory lesions using combined FLI and MRI in living mice. Macrophages are strong phagocytic cells that engulf all types of small particles and digest them in their phagosomes [20]. Due to their strong phagocytic activity, macrophages can be easily labeled with NIR fluorescent magnetic nanoparticles and can be visualized with FLI and MRI in living mice. In this study, we demonstrated that NIR fluorescent magnetic nanoparticles are convenient and safe imaging probes for cell labeling. Excellent labeling efficiency was achieved by simple incubation of NIR fluorescent magnetic nanoparticles with primary macrophages harvested from peritoneal fluid. More importantly, the cell labeling procedure with NIR fluorescent magnetic nanoparticles did not affect proliferation or phagocytic activity of primary macrophages at a concentration of 0.2 mg/ml NIR fluorescent magnetic nanoparticles, which is a commonly used concentration for *in vivo* studies.

We tracked macrophage migration to acute inflammatory lesions with NIR fluorescent magnetic nanoparticles and combined imaging with both FLI and MRI. To monitor macrophage migration to inflammation sites, an acute inflammation model induced by CG was developed in immunocompetent mice for this study. CG has frequently been used to induce experimental inflammation, arthritis, and chronic pain in animal models [21]. Nuclear medicine imaging with [^{18}F]FDG PET has been commonly used to demonstrate the inflammation status in living animals [18]. The intense uptake of [^{18}F]FDG was observed in CG-injected footpads using animal PET/CT, and subsequent histological analysis of inflammatory lesions confirmed the infiltration of acute inflammatory cells as well as macrophages.

As expected, early distribution of labeled macrophages was observed in the lung within 1 h after infusion of the cells (data not shown) and was still detected after 24 h with FLI. In contrast to the FLI findings, the distribution of macrophages in the lung was not demonstrable with MR imaging at 3 and 24 h, which may be attributable to the low target sensitivity rather than FLI in MR imaging [22, 23]. The sensitivity of FLI (not well characterized, but likely to be 10^{-9}–10^{-12} mol/l) is much higher than that of MR imaging (10^{-3}–10^{-5} mol/l) [24]. After induction of inflammation with the CG solution, migrating macrophages were

distinctly observed at inflamed sites at 3 h with *in vivo* FLI. The activity of FLI in inflammatory lesions increased until 6 h, whereas the decrease in FLI signals occurred at 24 h after inflammation induction. Similar to *in vivo* FLI findings, T_2*-weighted MR imaging showed the migration of infused macrophages in the inflamed footpads at 6 and 24 h, but early migration of infused macrophages to inflamed lesions was not visualized at 3 h after inducing inflammation. However, accurate localization of migrated macrophages was possible with T_2*-weighted MR imaging because the anatomic resolution of MR imaging is superior to that of FLI. In this study, we also demonstrated that our established technique for macrophage tracking with NIR fluorescent magnetic nanoparticles is feasible to evaluate the therapeutic efficacy of anti-inflammatory drugs in mice with inflammatory lesions. DEX is a potent anti-inflammatory drug that has been shown to modulate inflammation occurring at multiple levels within the immune and inflammatory systems [25]. *In vivo*-combined FLI and MRI successfully revealed the inhibition of macrophage migration to inflamed lesions in the DEX group within 3–6 h post-inflammation induction, and the inhibitory effect of DEX was monitored during follow-up imaging. In contrast, migrated macrophages labeled with our nanoparticles were clearly detected at inflamed footpads in the vehicle group. The results of *in vivo* imaging are well-matched with *ex vivo* FLI of excised organs as well as confocal fluorescent microscopic analysis of the excised inflamed tissue.

The potential use of our multimodal nanoparticles as an imaging probe for cell tracking has been previously suggested. Park et al. showed that this probe does not affect cell proliferation, surface markers, or morphological phenotypes of human cord blood-derived mesenchymal stem cells (MSCs), and these authors succeeded in revealing the distribution of infused MSCs in living mice with combined FLI and MRI [12]. Recently, a group reported that they successfully monitored the migration of MSCs to osteochondral defects in mice using an osteochondral repair model from days 1 to 14 [14]. However, there has been no previous report on the labeling of primary macrophages with NIR fluorescent magnetic nanoparticles as an FLI/MRI-compatible imaging probe. Specifically, no studies have investigated tracking labeled primary macrophages in living mice with inflammation while also using combined FLI/MRI, and further, no studies have monitored the therapeutic effects of anti-inflammatory drugs by using macrophages labeled with NIR fluorescent magnetic nanoparticles.

There are a few issues that should be addressed in our study. First, although our study focused on an animal model with acute inflammation, it is not clear whether the results of this study can be further extended to chronic inflammatory disease. We are trying to expand further our technique with NIR fluorescent magnetic nanoparticles to various inflammation models, including chronic inflammation, infectious abscesses, and arthritis. Second, contrary to reporter imaging techniques, *in vivo* imaging with NIR fluorescent magnetic nanoparticles cannot distinguish live or dead cells among infused cells or reveal the cellular proliferation status, which is an essential aspect of *in vivo* imaging for long-term follow-up study of cell tracking in living organisms. Third, each imaging method was performed with different imaging devices, which may have led to some inaccuracies in the imaging analysis because of difficulties in using the same position with the different instruments and co-registering different images. However, to date, there has not been any imaging device that could be used for combined MRI and FLI simultaneously. Fourth, inflammatory process was monitored by [^{18}F]FDG PET/CT imaging in this study. The value of FDG activity in inflamed lesion has been reported to have relationship with inflammatory process, mainly by the activated macrophage. But recently, it has been demonstrated that since FDG activity have been reported to not be as a direct surrogate for inflammation, there are some limitation of *in vivo* monitoring method of inflammatory process [26, 27]. So, during macrophage tracking study, the employment of inflammation-related specific imaging marker (such as integrin, MMP, neutrophil elastase, and cathepsin activity targeted imaging agent) in combination with [^{18}F]FDG PET/CT would be helpful to accurately understand the complicated biological mechanism of CG-mediated inflammation.

In summary, we successfully monitored primary macrophage migration toward inflammatory tissues using both FLI and MRI with NIR fluorescent magnetic nanoparticles in the same mouse. We also demonstrated the inhibitory effects of DEX, a potent anti-inflammatory drug, on macrophage migration to inflammatory lesions in immunocompetent mice. Combined FLI and MRI with NIR fluorescent magnetic nanoparticles is a technique that can be applied in cell trafficking studies and in the preclinical evaluation of new candidate compounds with various pharmacodynamic effects.

Acknowledgments. This work was supported by a National Research Foundation of Korea (NRF) grant funded by the Korean government (MEST, 2009-0078234); the National Nuclear R&D Program through the National Research Foundation of Korea (NRF) funded by the Ministry of Education, Science and Technology (No. 2012M2A2A7014020); a grant from the Korea Health Technology R&D Project, Ministry of Health & Welfare, Republic of Korea (A111345); grant no. RTI04-01-01 from the Regional Technology Innovation Program of the Ministry of Knowledge Economy (MKE) and the Kyungpook National University Research Fund (2013); a grant from the Medical Cluster R&D Support Project of Daegu Gyeongbuk Medical Innovation Foundation, Republic of Korea; and by the National Research Foundation of Korea (NRF) Grant funded by the Korean Government (MSIP) (2014R1A1A1003323).

Conflict of Interest. All authors declare no conflict of interest.

References

1. Burke B, Sumner S, Maitland N, Lewis CE (2002) Macrophages in gene therapy: cellular delivery vehicles and *in vivo* targets. J Leukoc Biol 72:417–428
2. Orlic D, Kajstura J, Chimenti S et al (2001) Bone marrow cells regenerate infarcted myocardium. Nature 410:701–705
3. Feldmann M, Steinman L (2005) Design of effective immunotherapy for human autoimmunity. Nature 435:612–619

4. Boehncke WH, Schon MP, Girolomoni G et al (2005) Leukocyte extravasation as a target for anti-inflammatory therapy—which molecule to choose? Exp Dermatol 14:70–80
5. Kelly M, Hwang JM, Kubes P (2007) Modulating leukocyte recruitment in inflammation. J Allergy Clin Immunol 120:3–10
6. Eisenblatter M, Ehrchen J, Varga G et al (2009) *In vivo* optical imaging of cellular inflammatory response in granuloma formation using fluorescence-labeled macrophages. J Nucl Med 50:1676–1682
7. Lee HW, Jeon YH, Hwang MH et al (2013) Dual reporter gene imaging for tracking macrophage migration using the human sodium iodide symporter and an enhanced firefly luciferase in a murine inflammation model. Mol Imaging Biol 15:703–712
8. Abreo K, Lieberman LM, Moorthy AV (1985) Distribution studies of 111In-oxine-labeled peritoneal mononuclear cells in tumor-bearing rats. Int J Nucl Med Biol 12:53–55
9. Seo JH, Jeon YH, Lee YJ et al (2010) Trafficking macrophage migration using reporter gene imaging with human sodium iodide symporter in animal models of inflammation. J Nucl Med 51:1637–1643
10. Nahrendorf M, Zhang H, Hembrador S et al (2008) Nanoparticle PET-CT imaging of macrophages in inflammatory atherosclerosis. Circulation 117:379–387
11. Lee JS, Kang HJ, Gong G et al (2006) MR imaging of *in vivo* recruitment of iron oxide-labeled macrophages in experimentally induced soft-tissue infection in mice. Radiology 241:142–148
12. Park KS, Tae J, Choi B et al (2010) Characterization, *in vitro* cytotoxicity assessment, and *in vivo* visualization of multimodal, RITC-labeled, silica-coated magnetic nanoparticles for labeling human cord blood-derived mesenchymal stem cells. Nanomedicine 6:263–276
13. Yin J, Kim JK, Moon JH et al (2011) hMSC-mediated concurrent delivery of endostatin and carboxylesterase to mouse xenografts suppresses glioma initiation and recurrence. Mol Ther 19:1161–1169
14. Lee JM, Kim BS, Lee H, Im GI (2012) *In vivo* tracking of mesenchymal stem cells using fluorescent nanoparticles in an osteochondral repair model. Mol Ther 20:1434–1442
15. Kim TH, Kim JK, Shim W, Kim SY, Park TJ, Jung JY (2010) Tracking of transplanted mesenchymal stem cells labeled with fluorescent magnetic nanoparticle in liver cirrhosis rat model with 3-T MRI. Magn Reson Imaging 28:1004–1013
16. Kim SM, Kim DS, Jeong CH et al (2011) CXC chemokine receptor 1 enhances the ability of human umbilical cord blood-derived mesenchymal stem cells to migrate toward gliomas. Biochem Biophys Res Commun 407:741–746
17. Ogawa M, Magata Y, Kato T et al (2006) Application of 18F-FDG PET for monitoring the therapeutic effect of antiinflammatory drugs on stabilization of vulnerable atherosclerotic plaques. J Nucl Med Off Publ Soc Nucl Med 47:1845–1850
18. Stumpe KD, Dazzi H, Schaffner A, von Schulthess GK (2000) Infection imaging using whole-body FDG-PET. Eur J Nucl Med 27:822–832
19. Hansch A, Frey O, Sauner D et al (2004) *In vivo* imaging of experimental arthritis with near-infrared fluorescence. Arthritis Rheum 50:961–967
20. Johnston RB Jr (1988) Current concepts: immunology. Monocytes and macrophages. N Engl J Med 318:747–752
21. Radhakrishnan R, Moore SA, Sluka KA (2003) Unilateral carrageenan injection into muscle or joint induces chronic bilateral hyperalgesia in rats. Pain 104:567–577
22. Cheon J, Lee JH (2008) Synergistically integrated nanoparticles as multimodal probes for nanobiotechnology. Acc Chem Res 41:1630–1640
23. Kang JH, Chung JK (2008) Molecular-genetic imaging based on reporter gene expression. J Nucl Med Off Publ Soc Nucl Med 49(Suppl 2):164S–179S
24. Massoud TF, Gambhir SS (2003) Molecular imaging in living subjects: seeing fundamental biological processes in a new light. Genes Dev 17:545–580
25. Yang YH, Morand EF, Getting SJ et al (2004) Modulation of inflammation and response to dexamethasone by Annexin 1 in antigen-induced arthritis. Arthritis Rheum 50:976–984
26. Brammen L, Palumbo B, Lupattelli G, Sinzinger H (2014) Is (18)F-FDG PET really a promising marker for clinically relevant atherosclerosis? Hell J Nucl Med 17:62–63
27. Palestro CJ, Love C (2012) Decreased sensitivity of (18)F-fluorodeoxyglucose imaging in infection and inflammation. Semin Nucl Med 42:261–266